International Conference on Space Optics—ICSO 2018

Chania, Greece

9–12 October 2018

Straylight of curved gratings: an interlaboratory comparison

Monika Kroneberger

Dana Tomuta

Andreas Mezger

Straylight of curved gratings , an interlaboratory comparison

Monika Kroneberger*[a], Dana Tomuta[b], Andreas Mezger[a,]

[a] *OHB Systems AG, Manfred-Fuchs-Str. 1, 82234 Wessling, Germany*
[b] *TEC-MMO, ESTEC, Keplerlaan 1, PO Box 299, NL-2200 AG Noordwijk, The Netherlands*

ABSTRACT

The accurate simulation of stray light is essential for the verification of the contrast requirements in optical instruments. In a spectrometer, the scattering from reflective gratings is difficult to characterize while contributing significantly to the overall system stray light and reduction of the spectrometer contrast.

Curved gratings also introduce higher straylight and difficulties in the verification of their straylight compliance. Scatterometers have to be adapted to the grating curvature and thus loose some of their performance.

While measuring a curved sample, this becomes part of the optical system of the scatterometer. For the AlbatrossTT and the CASI the system considering the curved sample has to be adapted to refocus the beam onto the detector. Additional aberrations modify the near angle limit, i.e. the smallest angle where the measured BRDF is higher than the system signature. Theoretical analysis of the scatterometer becomes necessary because the signature of the system is no longer directly measureable.

In addition, 2D BRDF measurement is adequate for characterization of a high polished optical surface or black coatings but deems to be insufficient to characterize all features of the grating scatter function.

3D measurement is essential to verify compliancy in all angular directions.

Small errors in the measurement procedure or measurement setup can lead to different results. Also every scatterometer setup has its own design driven limitations effecting near angle limit and resolution. To create reasonable results those limitations have to be carefully considered.

We present a set of measurements in two different laboratories with different scatterometers.

Keywords: optical gratings, BRDF, stray light, scatterometer, stray light requirement

1. INTRODUCTION

Stray light requirements for spectrometer gratings are defined in terms of equivalent surface roughness [1]. The required Biderectional Reflection Distribution Function (BRDF) is calculated as the scatter function of a smooth mirror with a defined roughness value. For an easy fit procedure this function is approximated by a Harvey-Shack function (see Figure 1-1) and fitted to the measured BRDF of the grating at the peak of the diffraction order at which the grating is designed to operate. (detailed discussion see [7] and [9]).
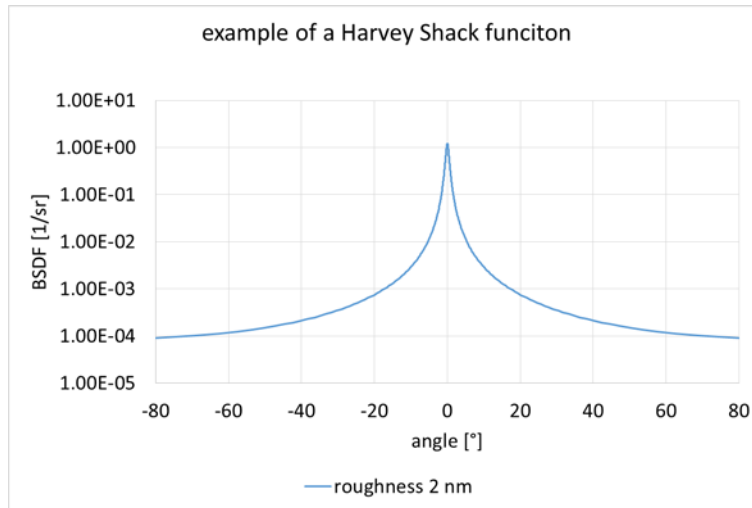
Figure 1-1. Example of a BRDF approximated by a Harvey-Shack function for a mirror with 2nm roughness at 532 nm wavelength

The fitted Harvey-Shack function is then compared to the Harvey-Shack function resulting from the requirement for compliancy.

The BRDF function measured by a scatterometer, such as the Albatross TT or the CASI, is expressed by the following equation, corresponding to the geometry illustrated in Figure 1-2:

$$\text{BRDF}(\theta_i, \theta_s, \phi_s) = \frac{dP_s(\theta_i, \theta_s, \phi_s)}{d\Omega_s P_i \cos \theta_s}$$

The incident angle is referred by θ_i. θ_s and ϕ_s refer to the azimuthal and tangential scattering angles, P_i is the power incident on the sample and P_s is the scattered power collected by the detector in the solid angle $d\Omega_s$.

Measuring the BRDF especially of gratings and curved samples with high reliability requires a deep understanding of the scatterometer setup and perfect alignment of the samples. Each scatterometer has its own limitations that need to be taken into account when analyzing the results.

Both scatterometer work with a focused beam on the detector and have to be refocused when measuring a curved sample to refocus the beam onto the detector. This change of the optical system introduces additional aberrations and changes the spot size and shape on the detector. For the measurement of roughness scatter, the near angle region is essential and the additional aberrations usually broaden the spot enlarging the near angle limit. For both systems, theoretical analysis is essential to identify the new limitations.

In this paper, we want to show the differences in the measurement with an AlbatrossTT and a CASI scatterometer based on two exemplary grating samples (one plane, one curved). The same samples were measured first with the CASI and then with the AlbatrossTT.

1.1 AlbatrossTT setup at OHB System AG

OHB System AG has an AlbatrossTT specially designed for near angle scatter measurement. In the nominal setup scatter can be measured down to 0.1° scatter angle. The two axes of the detector arm allow the scanning of the full hemisphere around the sample. Figure 1-2 shows the detector arm and the sample holder of the OHB AlbatrossTT with incident light direction and rotation axes.
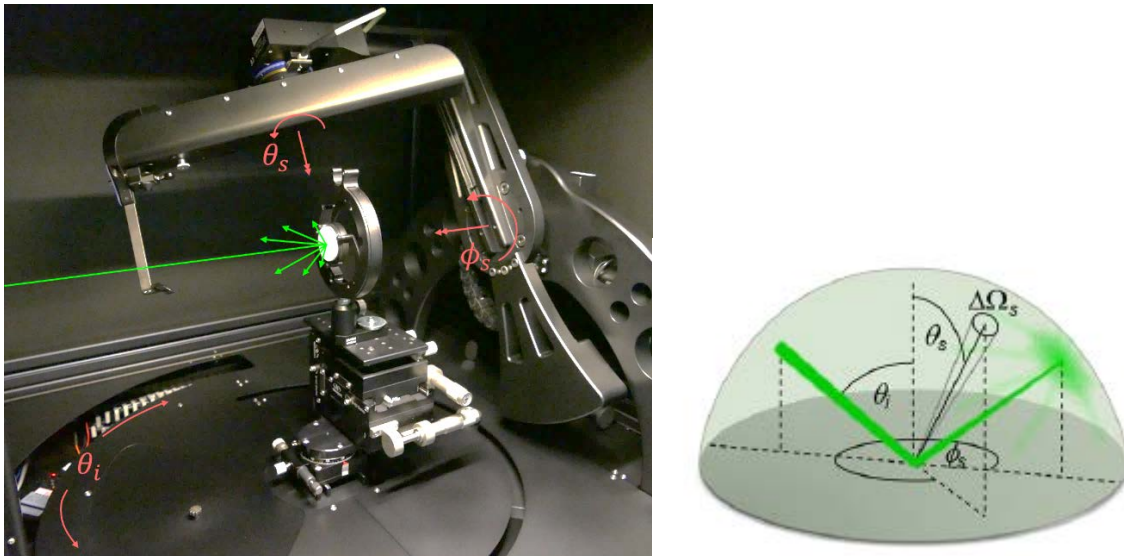
Figure 1-2.   Albatross TT and its measurement geometry (right figure extracted from the manual courtesy of Fraunhofer
        IOF)

This setup allows measurement of a 3-dimensional BRDF by varying θ_s and ϕ_s for a given incidence angle. The near angle limit is defined by the angle from the center of a reflection peak, where the scatterometer is able to differentiate between instrument signature and stray light from the test sample. The near angle limit depends on the optical geometry of the scatterometer and the sample under test. The instrument signature is the BRDF of the scatterometer itself. Every scatterometer and within the scatterometer every used source has it's own signature. The type of sample together with the signature of the used scatterometer and wavelength determines the near angle limit for this particular measurement.

1.2 CASI scatterometer set-up at ESTEC/ESA

The scatterometer available in Optical and Opto-Electronic Laboratory at ESTEC/ESA, is an Complete Angle Scatter Instrument (CASI) allowing the use of different laser sources raging from UV up to IR. The samples under test are mounted on stages capable of moving in X and Y direction and/or rotation as described in Figure 1-3. The incident angle can be set to any angle up to ~85° from surface normal. The detector sweeps around the sample in the incident plane measuring scattered and specular light. During the scan, the computer controls the gain and aperture changes through user-defined parameters. The CASI scatterometer is a classical scatterometer using a convergent beam on its best focus at the detector plane.
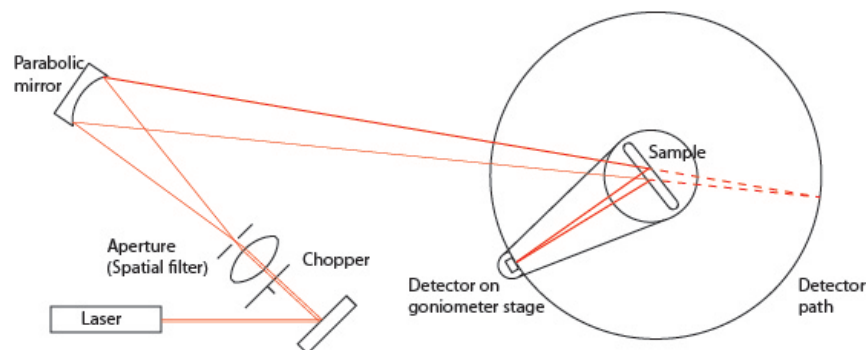

Figure 1-3:   Optical schematics of CASI

Compared to Albatross TT system, CASI has the advantage of easy accommodation of different light sources and some freedom in focusing at different goniometer radii, however one of the limitations being the BRDF measurement is only possible in one plane, the scattered plane.

The properties of the Albatross TT and the CASI setup are summarized in Table 1-1.

Table 1-1. Scatterometer properties.

	Albatross TT	**CASI**
Wavelength	532 or 1064nm	325, 532, 633, 780, 1064, 1600 and 2350-2450nm
θ_i	-90º to +90º	~ -90º to +90º
ϕ_s	-90º to +90º	fixed
θ_s	-180º to +180º	-180º to +180º
Angular resolution	< 0.02º	~ 0.001°
Dynamic range	13 orders of magnitude	10-12 orders of magnitude (λ dependent)
Near angle limit	0.1°	0.1°
Sample size	$< 100 \times 100$mm	No constrains below 200mm

2. SAMPLE DESCRIPTION

Two holographic gratings are measured in the two scatterometer setups:

- One flat grating, 1500 lines/mm

- One curved grating, 1500 lines/mm, convex with 207 mm radius

Both laboratories measured the same samples. After a first set of measurements at ESTEC, the samples were bagged and shipped to OHB System AG. Samples were delivered for the use in ISO 8 clean rooms.

Table 2-1 shows the list of samples.

Table 2-1: List of samples for measurement

Sample type	Samples	Measurement type
Grating curved (dd15ax_ bl7)	1 sample	2D BRDF with both scatterometers and 3D BRDF with AlbatrossTT
Grating flat (dd15ab)	1 sample	2D BRDF with both scatterometers and 3D BRDF with AlbatrossTT

The curved grating (convex) is circular with a diameter of 70 mm, the flat grating is rectangular with 60 x 40 mm.

The flat grating was adjusted in correlation with the incoming beam with regard to the indicated blaze direction on the backside of the grating.
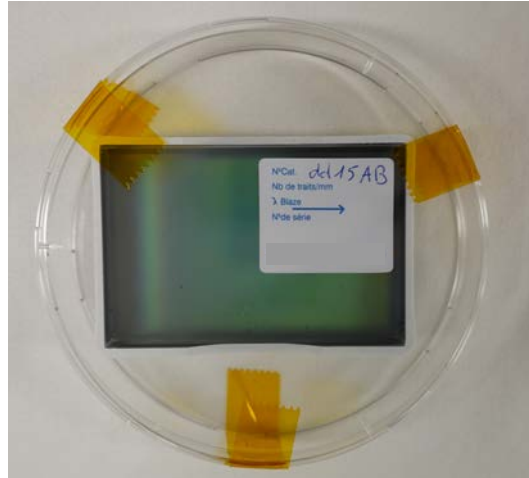
Figure 2-1:   Plane grating in transport packing with blaze arrow on the backside.

The curved grating was adjusted in correlation with the incoming beam with regard to the phase on the backside of the grating indicating the grating orientation.
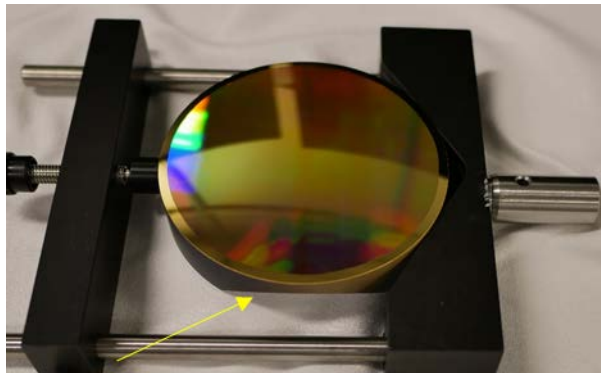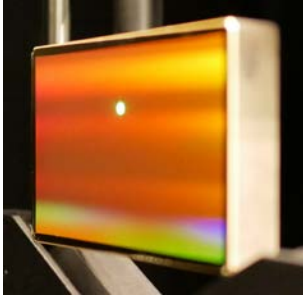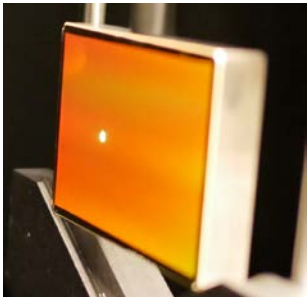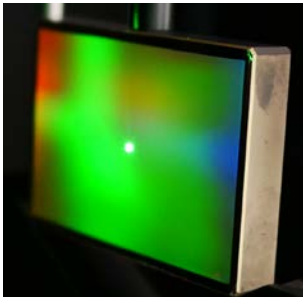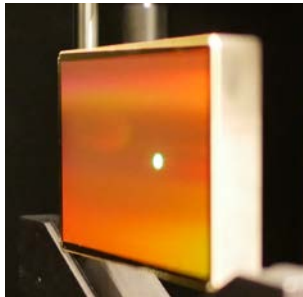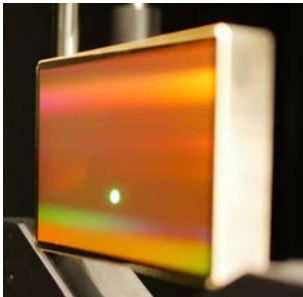

Figure 2-2:   Curved grating in mount for AlbatrossTT. On the lower side, the flat indicating the grating direction is visible.

3.   TEST POSITIONS

3.1 plane grating (dd15ab)

For the AlbatrossTT five measurement positions were defined: The middle of the grating and four points in cross configuration around it. For CASI, only one point of measurement was considered, at the middle, referred here, in Table 3-1, as Measure1.
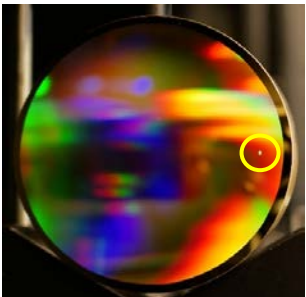
Table 3-1:   Name and position of measurement points.

Name of Measurement Point (X, Y-Coordinates in mm) and Image of Laser spot on the Test Position		
	Measure4 (15.00, 12.00)	
Measure2 (25.00, 5.00)	Measure1 (15.00, 5.00)	Measure3 (5.00, 5.00)
	Measure5 (15.00, -2.00)	

3.2 curved grating (dd15ax_ bl7)

For the AlbatrossTT three measurement positions were defined: The vertex, a point roughly in the middle between vertex and rim of the grating and a point close to the rim, all on the same vertical position. For CASI, only one point of measurement was considered, at vertex, referred here, in Table 3-2, as Measure1.

Table 3-2:   Name and position of measurement points. The yellow circle marks the laser spot on the grating surface.

Name of Measurement Point (X, Y-Coordinates in mm) and Image of Laser spot on the Test Position		
Measure1 (0.00, 0.00)	Measure2 (-13, 0.00)	Measure3 (-26, 0.00)

Both 2D and 3D measurement with AlbatrossTT scatterometer were done at exactly the same positions. An automated sample holder with position memory guaranties the reproduction of the measurement position with an accuracy of ± 0.05 mm (see capter 4.1).

4.   TOLERANCES, VERIFICATION ACCURACY

4.1 AlbatrossTT

BRDF measurements with the AlbatrossTT are accurate to within 10 % [6]. The variation of the scattering properties across the sample surface can be much larger than the uncertainty of the measurement system. The standard deviations from the three different test positions on the sample were calculated. The calculated relative standard deviations are presented in chapter 6.1 and are plotted as error bars in the diagrams.

As the monochromatic laser source creates speckle the measurements varies especially when using small apertures. This speckle pattern averages out when averaging over many different surface positions. The variation on a single spot depends on the spot size, focus, surface roughness etc. and is hard to predict. The signal variation is typically in a range of 20-50% for a 0.2mm aperture.

The uncertainty of the θ_i, θ_s and φ_s axes is roughly 0.01° especially when the axis direction of movement is reversed. The alignment of the axis relative to each other is roughly ± 0.02°. The offset between θ_s axis and θ_i axis is ~ 1 mm. The offset between Laser beam and φ_s axis is < 0.1 mm.

Position uncertainty on the sample is estimated with ± 0.05 mm depending mainly on the referencing process when determining the center of the sample. The illuminating laser spot has a diameter of approximately 3 mm. The Z-axis can be adjusted with an accuracy of approximately ± 0.03 mm. The angular adjustment allows an uncertainty of ± 0.07°, which is however limited by the aberrations of the illumination optics. The angular uncertainty of the sample positioner is roughly ± 0.01°. The rotation uncertainty around the sample center depends on the sample diameter. All uncertainties are related to the initial referencing of the sample w.r.t. AlbatrossTT coordinate system. The relative movements between different positions on the sample are much more precise.

4.2 CASI

According to the CASI SMS instrument specifications the following budgets applies:

1.   Total System Accuracy: 5%

2.   Total System Linearity: 2%

3.   Repeatability: 2%

However, these are too generic and need elaboration. The estimated uncertainty in measured BRDF (CASI) varies with the magnitude of the BRDF (in sr^{-1}) and therefore a break-down of uncertainty values can be used- see Table 4-1.

Table 4-1: Uncertainty budget for CASI measurements

BRDF graph value (sr^{-1})	Estimated Uncertainty (±%)
> 100	> 3
10-100	5
1-10	10
0.01-1	25
10^{-4} -0.01	50
< 10^{-4}	< 100

5. SIGNATURE DETERMINATION

5.1 AlbatrossTT

To measure curved samples, we need to refocus the scatterometer. In the nominal setup the beam is focused on the detector. With a non flat sample a refocusing has to be done to achieve again the focus on the detector. The "beam preparation unit" of the AlbatrossTT has a focusing unit, allowing the refocusing of the beam.

Once focused, we cannot use the setup without a sample with an appropriate curvature. This makes direct measurement of the scatterometer's signature without a sample impossible. In our case, we are interested in the near angle signature, which includes aberration and stray light from the scatterometer optics. There are two ways to obtain the near angle signature in a focused configuration (detailed discussion in [8]):

Indirect method

The signature of the system is simulated and measured for the standard configuration (appropriate for flat samples). The simulation has to be as close as possible to the correct stray light properties of all system components which is controlled by comparison of simulated and measured signature. When the best compliancy is reached, the refocused system is simulated with the same parameters and the result is a theoretical signature which should be close to the real instrument signature.

Direct method

It is also possible to replace the sample by a mirror with the same curvature and negligible scattering behavior. When using off the shelf components, the latter can be problematic. Especially for high quality space components the roughness of off the shelf products might be higher than the scatter of the samples and the measured signature will give no hint about the real near angle limit of the measurement. We recommend simulating the signature at least in addition to the measured signature.
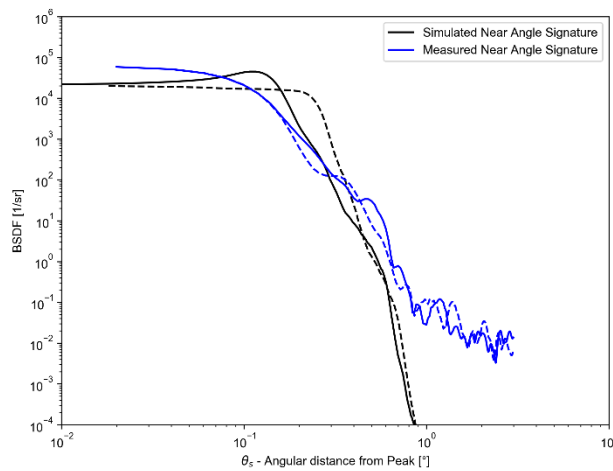
Figure 5-1:   Simulated (black) and measured (blue) signature for a refocused system. The scatter of the mirror used instead of the sample causes the higher values for scatter angles greater than 0.8°.

The simulated near angle signature is a combination of three contributors: optical aberrations in the scatterometer, scattering from the instrument itself and clipping by the detector field of view.

In the focused case, the aberration increases reciprocally with the convex radius of curvature of the test sample and the near angle limit increases. These results also illustrate a limitation of the measurement setup; namely, the impossibility of measuring scattering close to the specular direction (within the near angle limit) due to the width of the signature function.

5.2 CASI

Before starting any BRDF measurement campaigns, an instrument signature scan is taken, having no sample on the sample mounted yet in the set-up. The instrument signature is a measurement of the incident laser beam profile at the position of the detector where a point source is imaged with high F#. The instrument signature at the requested wavelength, e.g. 633nm, provides the information about the angle-dependent sensitivity of the instrument (noise-floor) and also gives an indication of the set-up limitations/aberrations present due to optical components within the set-up, mostly affecting the near-specular region –see Figure 5-2:. It is also important to mention that the footprint of the beam at the sample location –see Figure 1-3 is usually around 5mm in diameter.

The signature is valid to be used when measuring any flat optical component but will be no longer representative when there is an additional optical power from the sample to be measured. Ideally, a direct measurement of a curved blank sample having same optical power would be recommended as described above in 5.1.

It should be mentioned that due to the aberrations introduced by the convex grating, adjustments of the focusing beam are mandatory to reduce/minimize the gratings diffracted spot astigmatism at detector location. In addition, optical components of the set-up may be exchanged to reduce the beam footprint at the sample-measured position. Without entering all preparation details for the correct BRDF measurement, one should understand that changes on set-up will alter the instrument signature; e.g. re-adjusting the focusing stage. As the signature presented in Figure 5-2 is no longer valid, it still can be considered as indicative at least for the dynamic range.
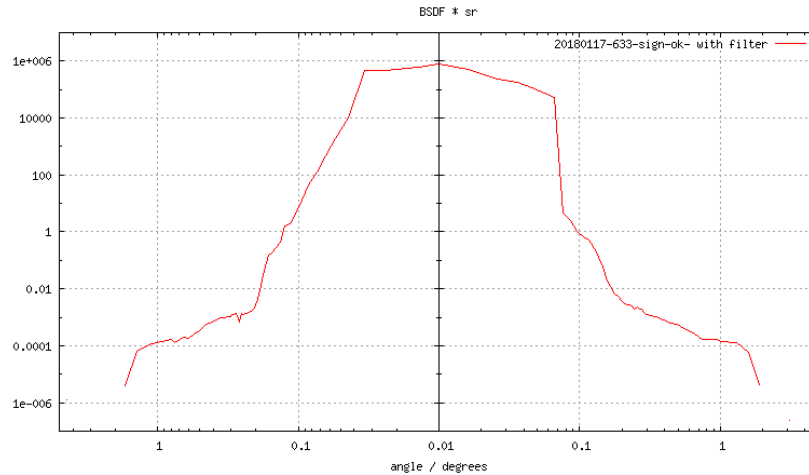
Figure 5-2: Measured CASI scatterometer signature at 633nm.

6. RESULTS

6.1 AlbatrossTT

6.1.1   Combination of Measurements with different Apertures

The 2D BRDF measurement with the AlbatrossTT has to be separated into sets with different aperture sizes. The step size and angular region for the single measurement have to be tailored to the measurement task. Small apertures are required for near angle measurements with a good angular resolution. Measurements of very faint signal require large apertures, which provide lower angular resolution but also accelerate the measurement. The measurements performed with different apertures (see Figure 6-1) need to be combined in order to be able to fit a BRDF curve of equivalent roughness.
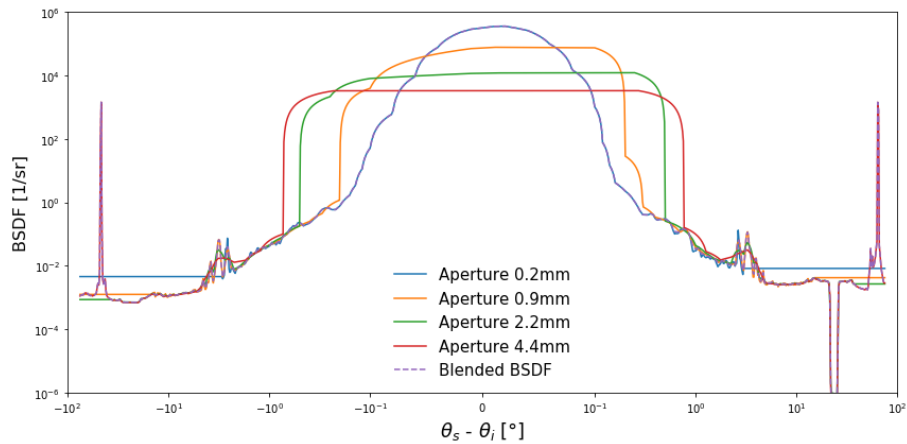

Figure 6-1: Measured BRDF of the plane grating dd15ab with four different apertures

To combine the measurements, they are multiplied by cross-fading functions. The sum of two overlapping cross-fading functions is always unity. As the BRDF usually follows a logarithmic function, the cross-fading functions are also defined to be logarithmic with respect to the scattering angle as shown in Figure 6-2.
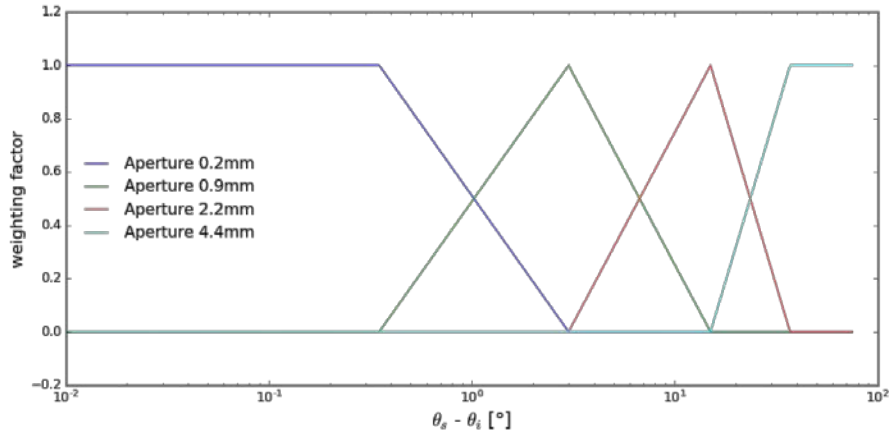
Figure 6-2 Cross-fading functions dependent on angular ranges used to combine measurements performed with different apertures. The angular limits are 0.35°, 3.0°, 15° and 37°.
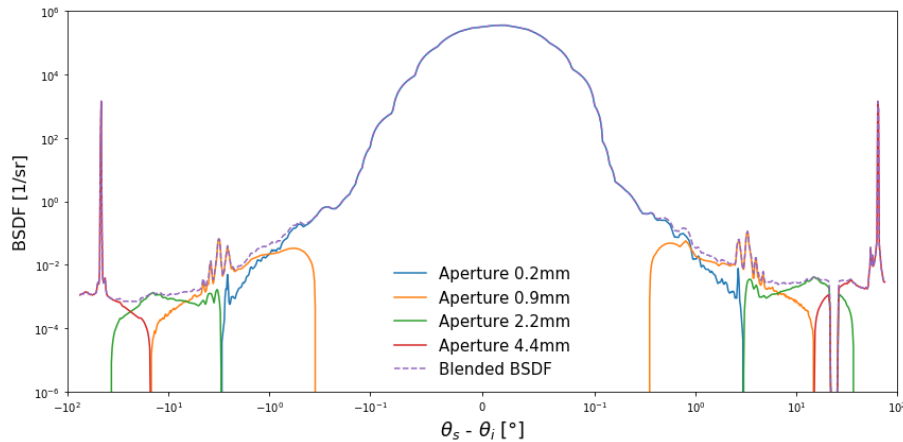

Figure 6-3 Measurements with different apertures of the plane grating dd15ab multiplied with their corresponding cross-fading function. The dotted line showing the resulting sum of the four curves on the graph.

Figure 6-3 shows that the combination of the four measurements with different apertures is not introducing any artefacts, but reducing speckle effect to an acceptable minimum and avoiding measurements to be noise limited at the same time.

6.1.2   2D measurements

The measurements were carried out at one wavelength in the visible range (532nm). Result of the measurements is the BRDF of the sample in dependence of the scatter angle in one dimension ($-85°<\theta_s;<85°,\varphi s=0$). The measured scatter plane is selected to be identical to the diffraction plane of the grating. I.e. the diffraction peak maxima are all in the measured BRDF. The Angle of Incident (AOI) i.e. the incident laser beam onto the surface of the sample is 35°.

6.1.2.1   plane grating (dd15ab)

The following 2D measurements have been captured at five different locations (see Table 3-1) on the sample and with four different apertures (see Figure 6-2). The following graphs show the raw measurements blended for the four apertures in different θ_s angle ranges. The measurements of the five different locations are averaged and the standard deviation is calculated and displayed as grey area.

The near angle range of +/- 1° and the angle range of +/-10° around the -1st diffraction peak are chosen to show the relevant angular area for system stray light. The graphs are logarithmic in the BRDF axis and linear in the angular axis.
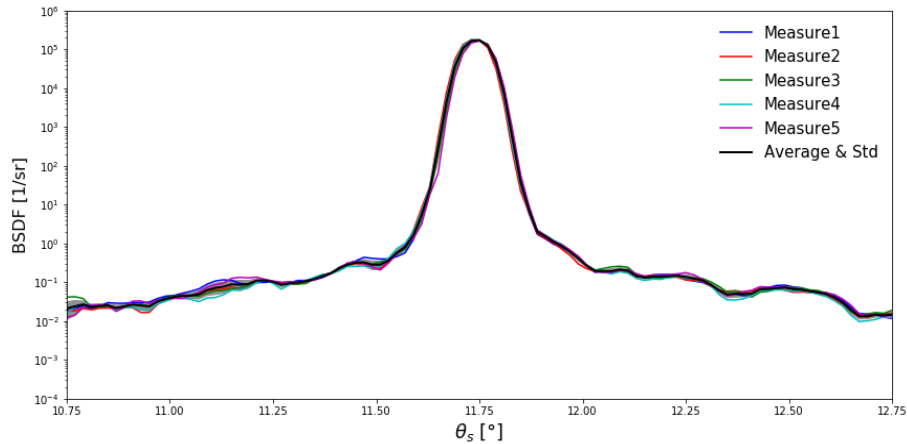
Figure 6-4:   Near angle range (+/- 1°) of all three measurements compared

The near angle range (see Figure 6-4) shows only the diffraction peak and the different speckle patterns of the measurements. No secondary peaks can be distinguished. Also the five measurement points show high conformity. In the wider range of +/-10° (see Figure 6-5) the comparison of the five measurements shows clearly distinguishable peaks in the range of 3° to 5° angular distance to the diffraction peak on both sides for some of the measurements. The size of the standard deviation shows that two of the peaks are present in all measurement points and thus tend to be valid for the full grating surface. The other three peaks are only present in some of the measurements and thus will probably average out over the full aperture of the grating. The peaks have a BRDF value of roughly 5E-3 1/sr compared to a peak value of roughly 1E4 (six orders of magnitude lower).
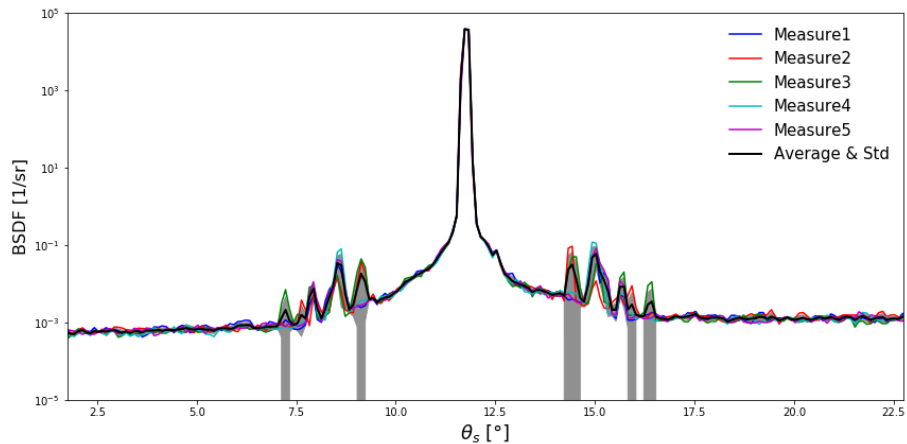

Figure 6-5:   Angle range (+/- 10°) of all three measurements compared.

In Figure 6-6 some additional features can be seen only for the -2nd diffraction order. These are most likely outside the angular range critical for the spectrometer and again in the range of six orders of magnitude lower than the nominal diffraction order. In between the diffraction orders the BRDF is clean of additional features in the 2D measurement.
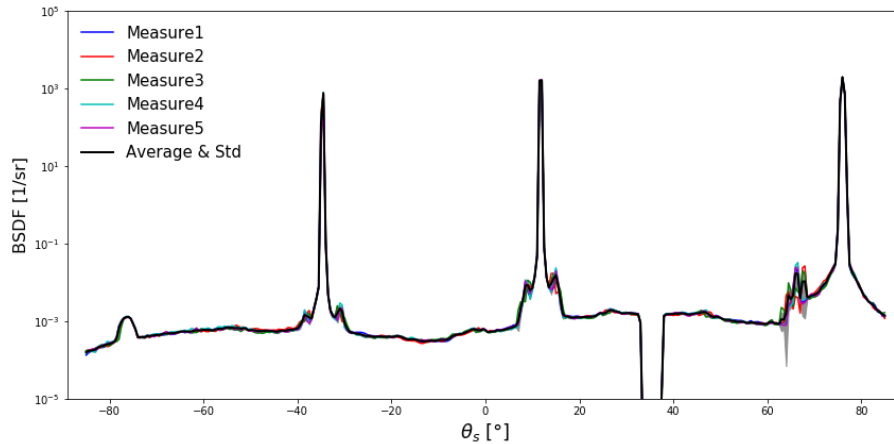
Figure 6-6:   Full 2D BRDF for all three measurement points compared.

The system signature of the AlbatrossTT in standard configuration was measured without any sample. Figure 6-7 shows the comparison of the averaged BRDF and the system signature. BRDF values can be extracted from the measurement starting at 0.12° from peak center (crossing point of signature and measured BRDF). The shoulder in the signature is roughness scatter from the folding mirror of the detector arm.
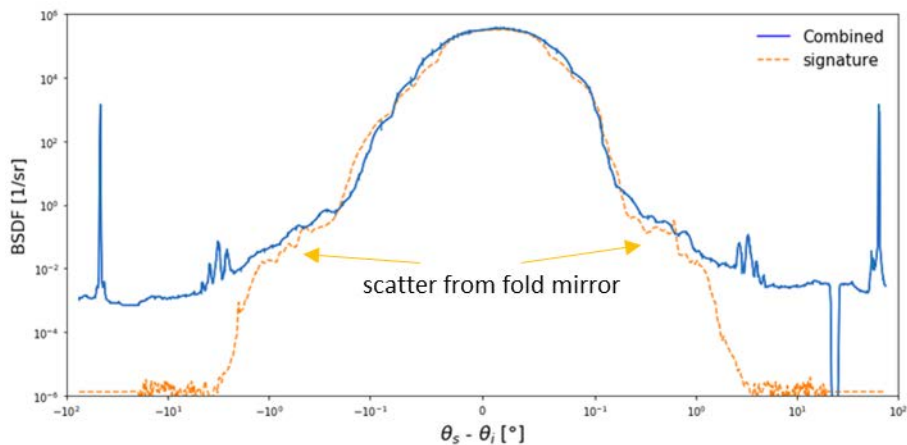

Figure 6-7:   Blended BRDF and signature measured at standard configuration

Fitting a Wein roughness to the measured BRDF of the grating leads to different equivalent roughness values for different angular areas (see Figure 6-8). The equivelant roughness is in between 1.3 and 2.3 nm and in the large angle range the scatter is almost lambertian like with 0.4% TS.
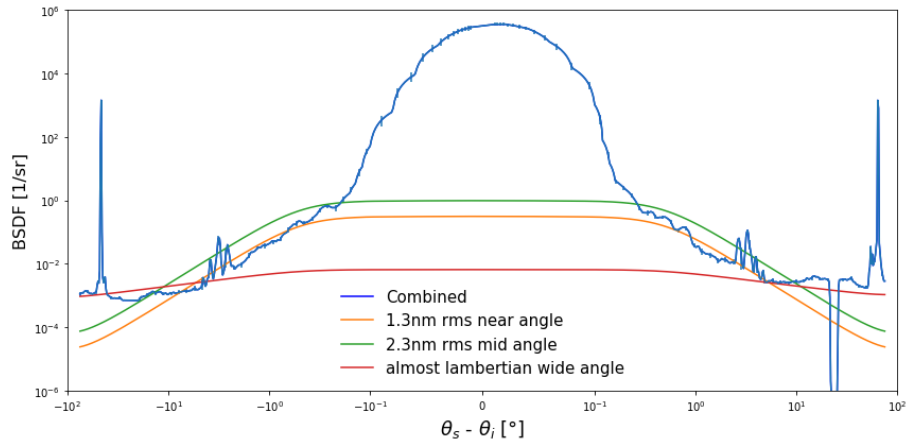
Figure 6-8:   Measured BRDF of the grating and fitted equivalent roughness functions

6.1.2.2   curved grating (dd15ax_ bl7)

The following 2D measurements have been captured at three different locations (see Table 3-2) on the sample and with four different apertures (see Figure 6-2). The following graphs show the raw measurements blended for the four apertures in different θs angle ranges. The measurements of the three different locations are averaged and the standard deviation is calculated and displayed as grey area.

The near angle range of +/- 1° and the angle range of +/-10° around the -1st diffraction peak are choosen to show the relevant angular area for system stray light. The graphs are logarithmic in the BRDF axis and linear in the angular axis.
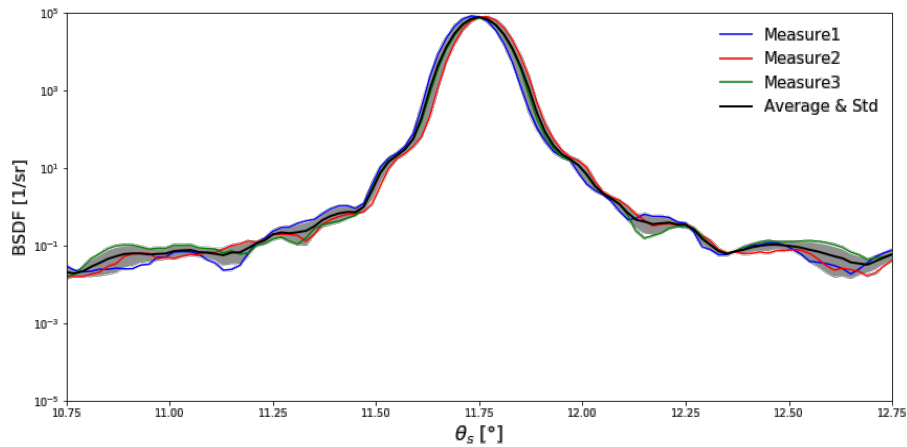

Figure 6-9:   Near angle range (+/- 1°) of all three measurements compared

The near angle range (see Figure 6-9) shows only the diffraction peak and the different speckle patterns of the measurements. No secondary peaks can be distinguished. In the wider range of +/-10° (see Figure 6-10) the comparison of the three measurements shows clearly distinguishable peaks at roughly 4° and 7° angular distance to the diffraction peak on both sides for some of the measurements.
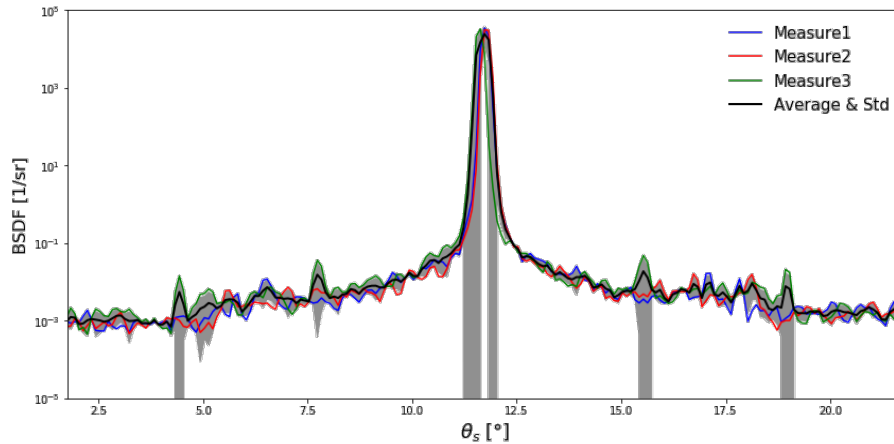
Figure 6-10:   Angle range (+/- 10°) of all three measurements compared.

In Figure 6-11 some far off features can be seen that will most probably not affect the instrument the grating will be used for.
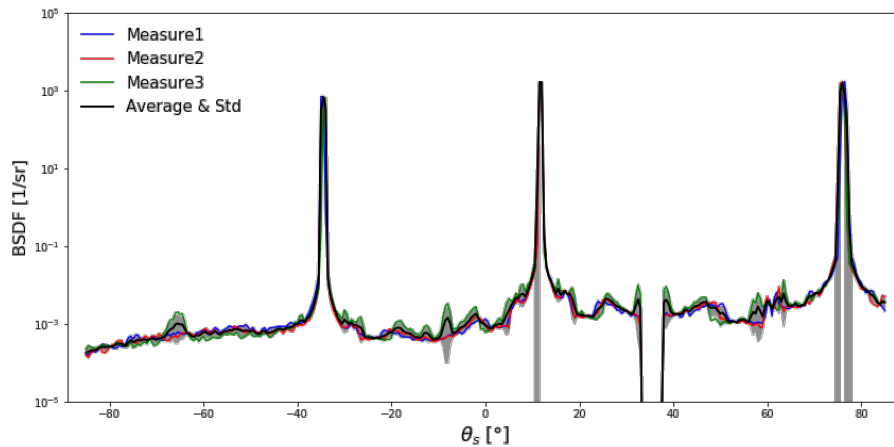

Figure 6-11:   Full 2D BRDF for all three measurement points compared.

The signature was measured at a silicon lens with equal optical radius as the grating. Figure 6-12 shows the drawback of this method. The roughness of the lens is equal or a little larger than the equivalent roughness of the grating. The two graphs cross at roughly 1° but the theoretical near angle limit for this configuration is 0.6°. A theoretical analysis with zemax of the illuminating optics with the sample is necessary to determine the correct near angle limit.
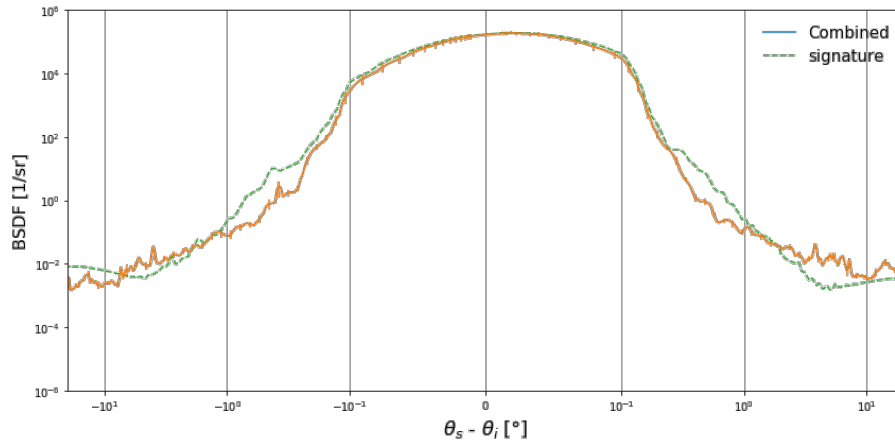
Figure 6-12:   Blended BRDF and Signature measured at a lens with equal optical radius

Fitting a Wein roughness to the measured BRDF of the grating leads to different equivalent roughness values for different angular areas (see Figure 6-13). The equivelant roughness is in between 2.3 and 3.8 nm and in the large angle range the scatter is almost lambertian like with 5% TS.
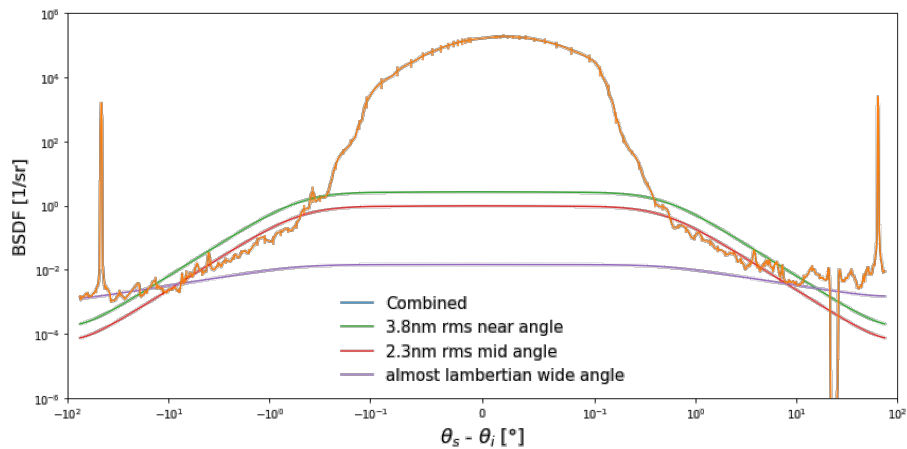

Figure 6-13:   Measured BRDF of the grating and fitted equivalent roughness functions

6.1.3   3D measurement

To determine the scatter patterns around the diffraction peak (-1st order), each point was also measured in 3D. Measurements were carried out according to Figure 6-14 to best sample the angular area of 7.5° around the peak. Three different scan regions (colored red, green and blue in Figure 6-14) are defined to guarantee equal scan distance for the complete measurement. The circle defines the angular area of interest. The number of scan regions and the step sizes and angular ranges for each scan region are calculated for the distinct parameters of the measurement.
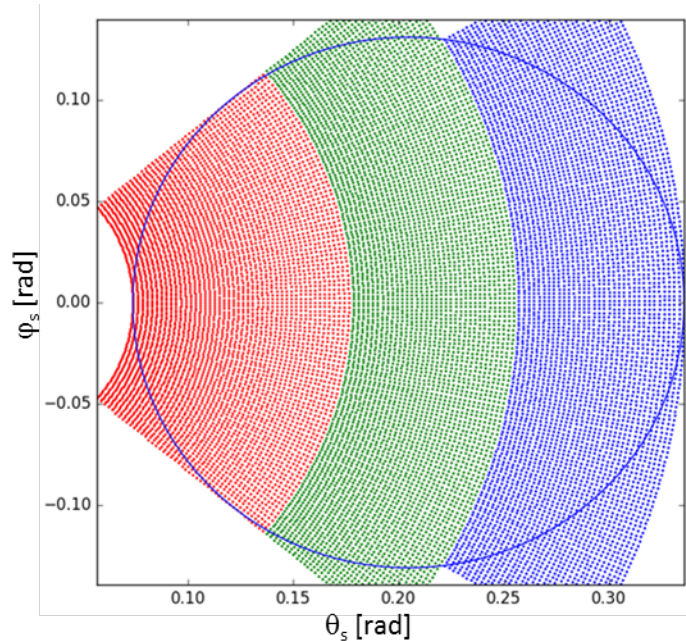

Figure 6-14:   Scan layout for the 3D measurement for optimal sampling of the angular area around the -1st diffraction order. Each dot is one detector position.

6.1.3.1   plane grating (dd15ab)

The following pictures (see Figure 6-15) show the five 3D measurements of the plane grating. Ringlike structures and faint peaks are visible. Those secondary features are most likely produced by the holographic setup. The reduction of those unwanted features is limited by optical coating quality and the optical setup of the holographic system.

The plane grating shows satellites only at the measurement points off center. The center has better performance than the outer areas of the grating. In total the performance of the grating in terms of straylight is good. The measurement shows that the secondary features vary over the grating surface. On the other hand, the BRDF is mostly isotropic except for the rings and can be approximated by the 2D BRDF averaged over all measurement positions.
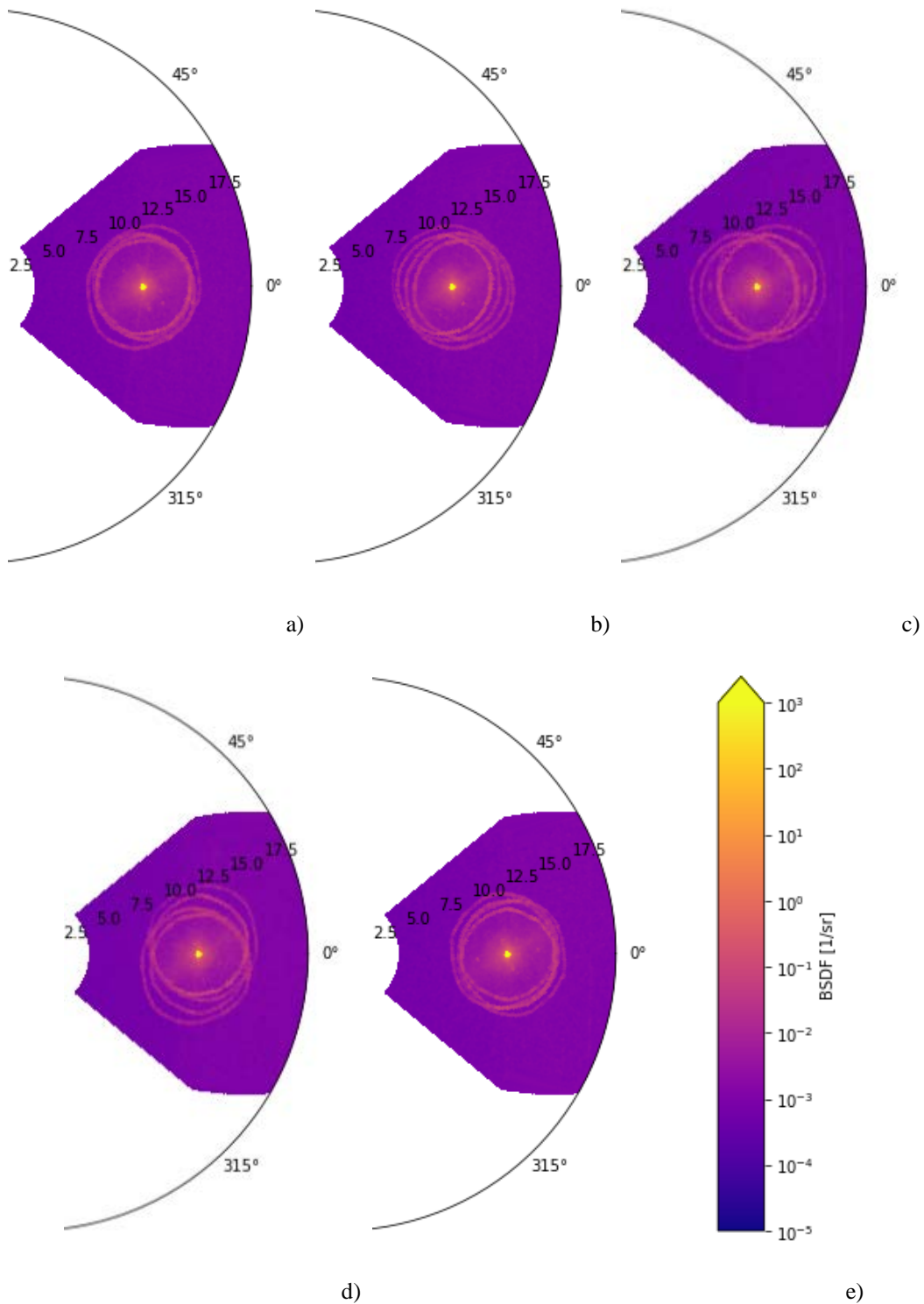
Figure 6-15:   3D measurements of measurement points 1 to 3. The center (point 1, a) shows the best performance, the two points to the left and right of the center show more secondary structures.

6.1.3.2   curved grating (dd15ax_ bl7)

Measurement showed that the grating has the best performance at the vertex and gains secondary effects with distance to the vertex (see Figure 6-16).

All three measurement positions show some satellites, the vertex only close to the peak, all others in addition on various positions in the vicinity of the peak. The intensity of those features is in the range of roughly 2E-2 1/sr compared to roughly 5E4 1/sr for the diffraction peak. The scatter performance is a little worse than for the plane grating but still good. The degrading to the edge of the grating is more pronounced than for the plane grating.

The secondary features have very low intensities and will most likely not contribute to system level straylight.

The BRDF is again mostly isotropic except for the secondary features and can be approximated by the 2D BRDF averaged over all measurement positions.

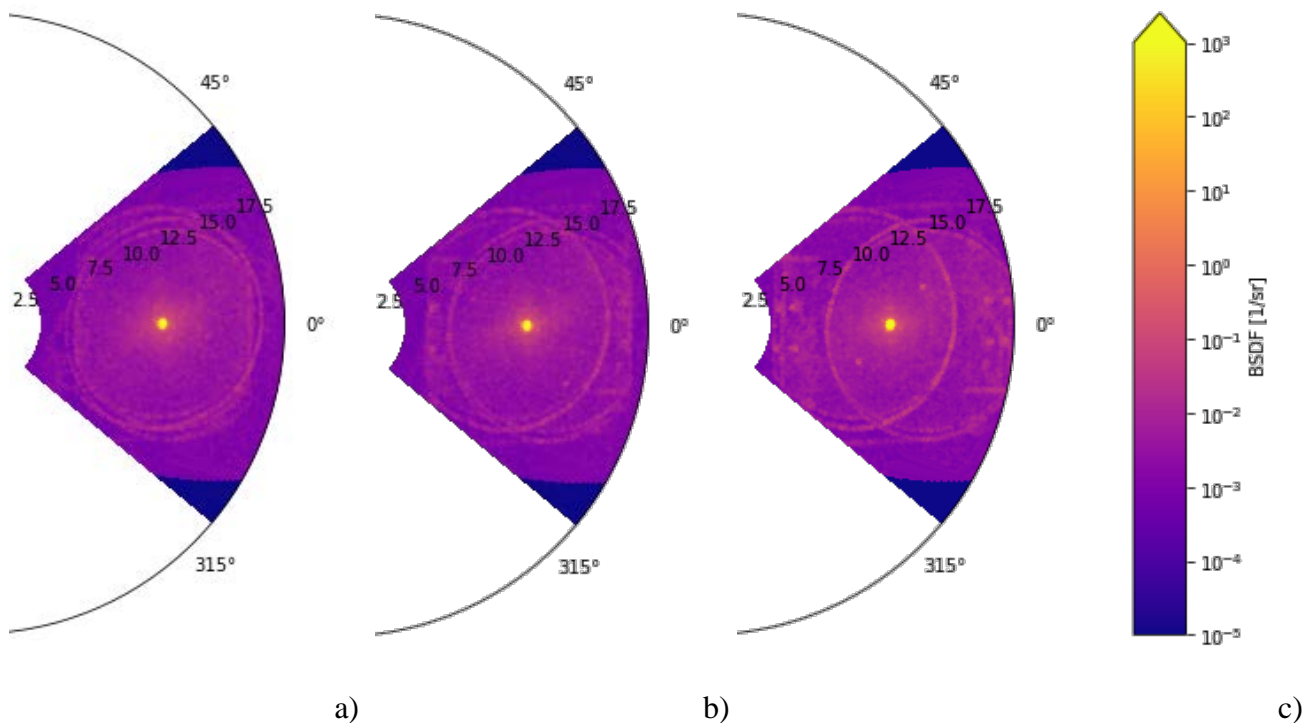a)   b)   c)

Figure 6-16:   3D measurements of measurement points 1 to 3. The vertex (Measure1, a) shows the best performance, the point closest to the rim (Measure3, c) the most secondary structures.

The 3D measurement was only carried out +/- 7.5° around the -1st diffraction order due to time limitation. The ring like features are accompanying all diffraction orders as can be seen in Figure 6-17.
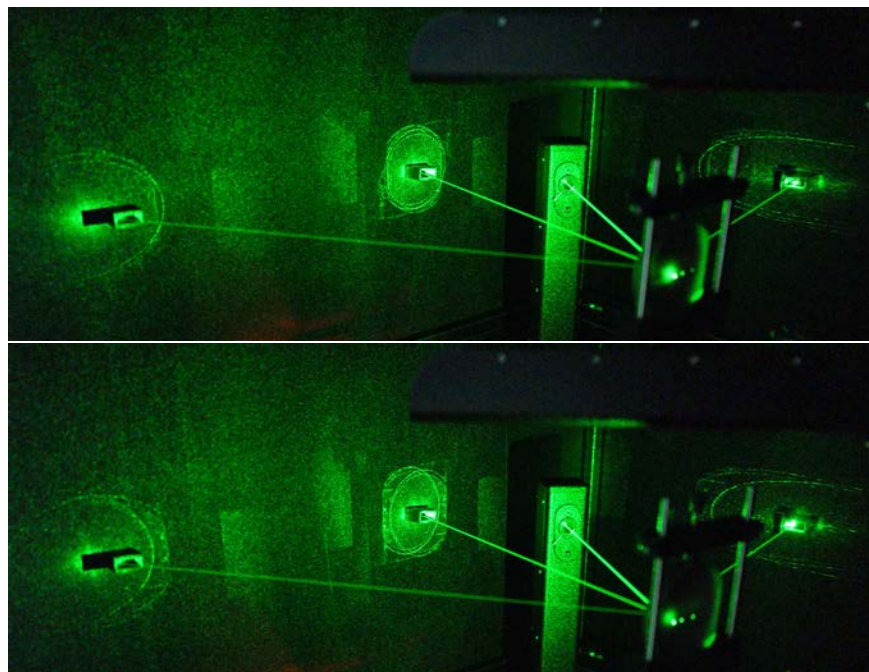
Figure 6-17:   Overexposed picture of inside of Albatross with curved grating illuminated with AOI 35°. All diffraction orders show ring features around the peak. Two different illuminated points on the grating surface.

6.2 CASI

CASI set-up has only the possibility of measuring 2D BRDFs, namely in the scatter plane. Gratings require additional efforts to be correctly aligned in the set-up to secure a correct BRDF measurement along the scatter plane. As first, its zero order is aligned in auto-collimation with the incoming laser beam as well as the other diffraction orders should be part of the detection plane. Independent of the sample to be measured, CASI has the advantage of having the possibility in choosing different aperture sizes in one measurement using a simple script command. The same principle for the aperture size applies as for Albatross TT see 6.1.1, by choosing small apertures with a high angular resolution for the near specular region. Both gratings as presented in Table 2-1 were measured only in the scatter plane/diffraction plane using a well-defined set-up configuration. The Angle of Incidence (AOI) referred here represents the angle of the incident laser beam onto the surface of the sample. The AOI is usually computed using Zemax simulation and should be compliant to the grating orientation in the instrument they are designed for. BRDF measurements were taken for both samples using an AOI of 35°. In addition, the curved grating was measured using an AOI of 20° and the BRDF results will be hereafter discussed.

6.2.1   plane grating (dd15ab)

Figure 6-18 shows the BRDF measurement of the flat grating dd15ad along the spectral direction. Note few features/satellites present in the BRDF as the scatter angle comes closer to the near specular direction. The symmetric feature, present at about 4° represents a small faint ring of stray-light having a scatter BRDF value of $7\text{-}8\text{x}10^{-2}$ compared to the grating scatter/straylight level of approximately $2\text{x}10^{-2}$, thus little contributing to the straylight of the grating. The asymmetric satellite, present about 0.65° only on the left side of the BRDF from Figure 6-18: unfortunately is an artifact of the laser source having a small intensity secondary line at about 640nm and therefore should be excluded from straylight assessment.
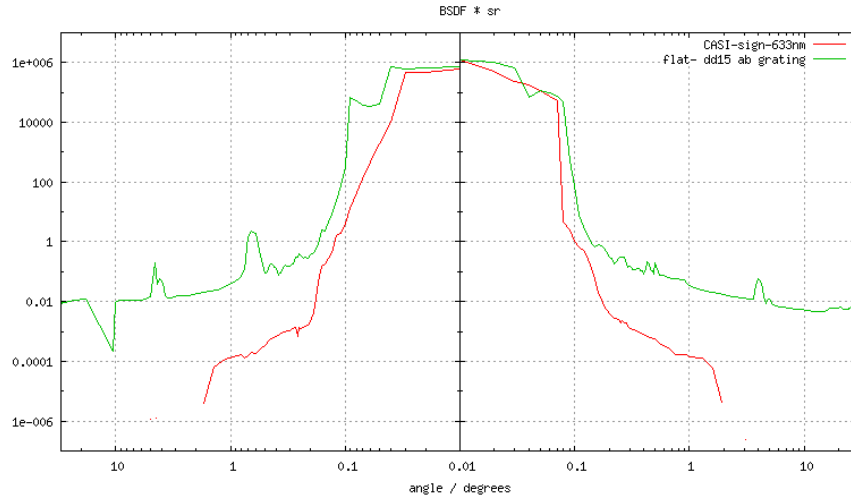
Figure 6-18: BRDF of flat grating dd 15ab

6.2.2   curved grating (dd15ax_ bl7)

The curved grating dd15ax_bl7 was measured in two different set-up configurations, for an AOI=35° as well as for an AOI=20°. Changing the AOI in the measurement configuration required also a change of the distance between the sample and detector, possible with CASI set-up. Refocusing the astigmatic beam, generated by the optical power of the grating, was done for each measurement configuration differently. A shorter distance to detector is required for the AOI=20° configuration. Figure 6-19 presents the BRDF results for those two particular configurations. One can notice that independent of the BRDF set-up measurement configuration, the stray-light level of the grating is within the accuracy of the measurement almost the same. The advantage of the close incident angle configuration is the possibility of mapping the scatter properties in the near specular region, as seen from Figure 6-19. Within the CASI sensitivity and the BRDF measurement configuration, no other features have been observed. The extra features present in the BRDF measurements are glitches of the CASI S/W or simply due to the obscuration region of the detector.
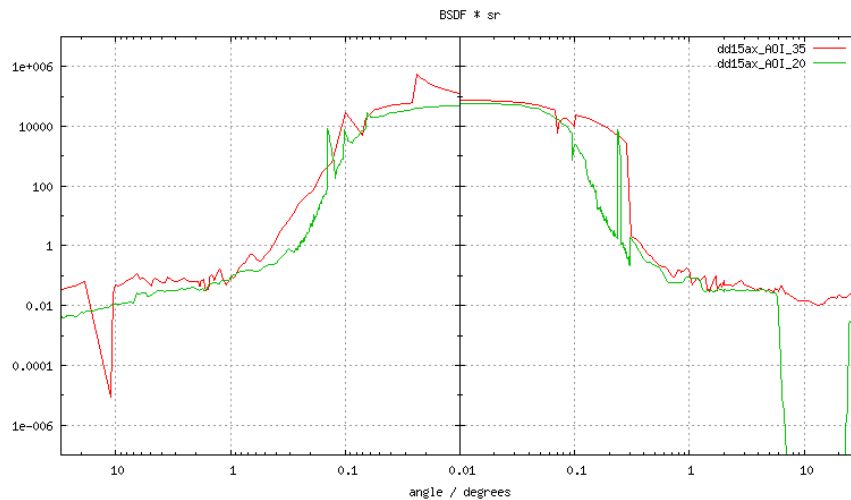

Figure 6-19 BRDF of curved grating dd15ax_bl7 measured in two different configurations.

6.3 Comparison of Measurements

The 2D measurements for the plane and the curved grating were post processed with the same routine to show the differences in the two measurement methods. Looking at the plane 2D curves no big differences can be seen. Both laboratories measured with similar tolerances and results.

The AlbatrossTT measurements are smoother due to the averaging over five (Figure 6-20) and three (Figure 6-21) measurement positions and the cross fading in between apertures. Changing apertures from one angle to the next can introduce steps in the measured BRDF.
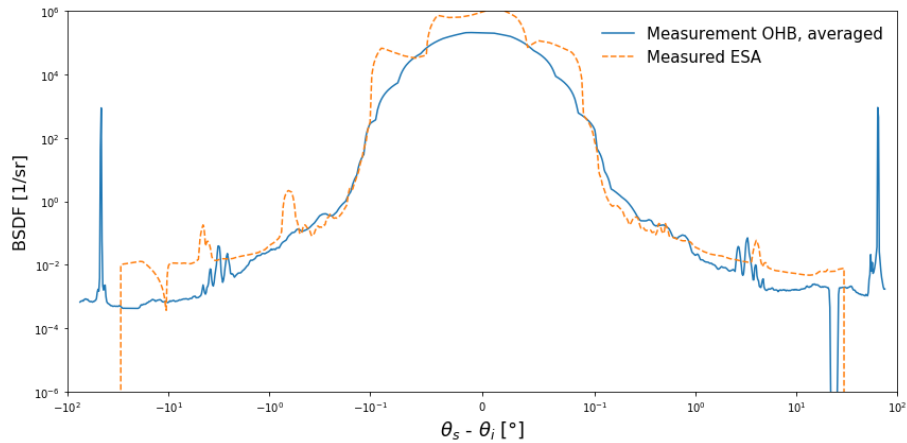

Figure 6-20:   Measurements of plane grating in different laboratories.

In Figure 6-20 the average over five measurement positions leads to four peaks in the range of 3 to 5° angular distance of the diffraction peak for the AlbatrossTT measurements whereas the CASI only measures the one ring present at the one chosen measurement position. Relevant for the system the grating will be used for is the averaged BRDF over the complete active aperture of the grating. Measuring many surface points and averaging the BRDFs gives results closer to the overall average.
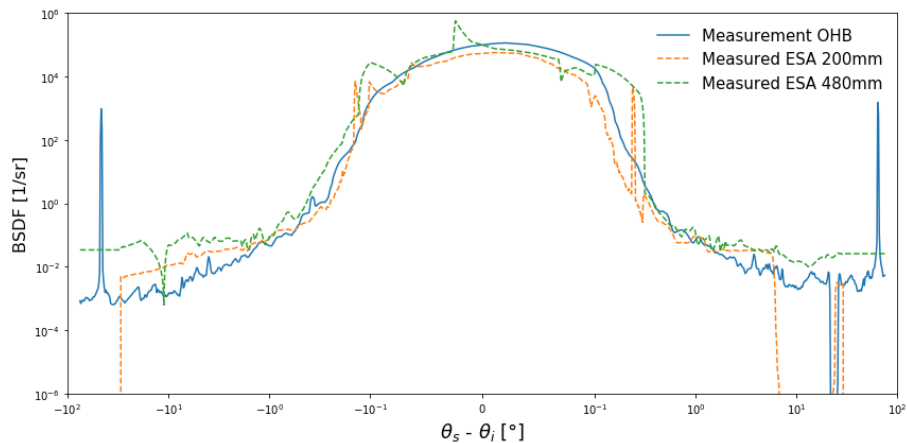

Figure 6-21:   Measurements of curved grating in different laboratories and configurations.

For the curved grating (Figure 6-21) the ring features are low power and not detectable in the single BRDF plot. The comparison of the CASI and AlbatrossTT measurements shows similar results. The measurement with 200 mm detector arm length and AlbatrossTT measurement with 250 mm detector arm length are in good agreement, the calculated roughness values of both laboratories are 2.3 to 3.8 nm equivalent roughnes at AlbatrossTT and 3.5 to 4 nm equivalent roughness for CASI .

The display of different measurements at different positions with deviation gives a hint to additional features and separates them from speckles. The automated sample holder with the possibility to repeat measurements at exactly the same position with different parameters at AlbatrossTT opens the possibility for this comparison (see Figure 6-22). Still only a 3D measurement can fully describe the BRDF and distinguish between peak and ring like features. Figure 6-23 shows the averaged BRDF of the five measurement positions of the plane grating. Rings and satellites are still visible but blurred.
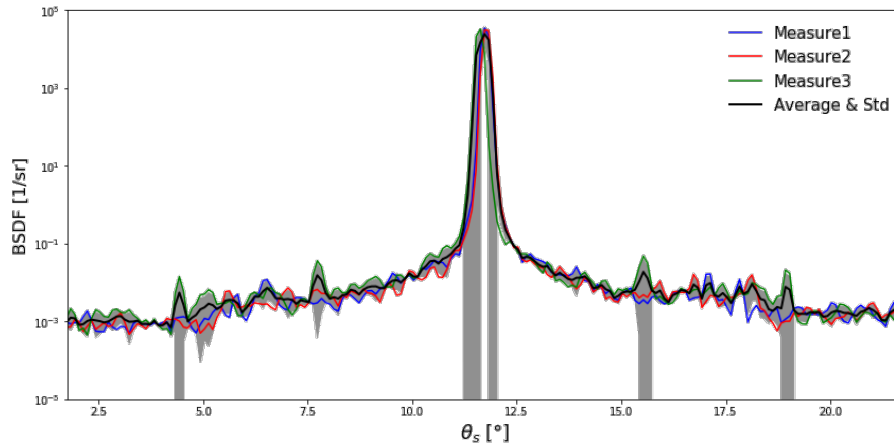

Figure 6-22:   Angle range (+/- 10°) of all three measurements of curved grating compared. The standard deviation separates speckles from diffraction features.
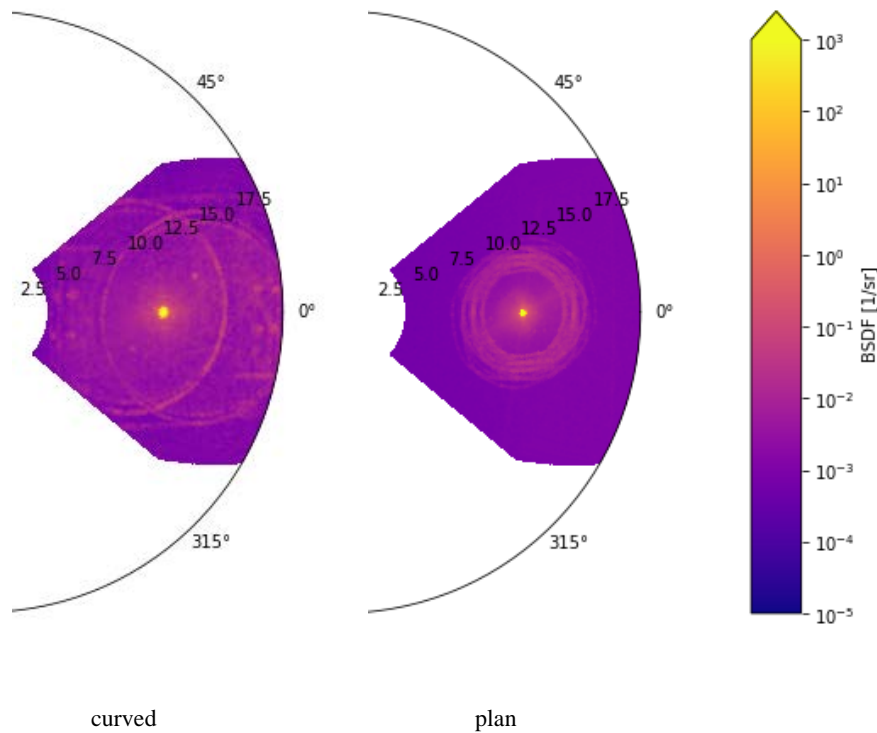

curved   plan

Figure 6-23:   3D BRDF averaged over three and five measurement positions respectively. Rings and satellites are still visible but blurred.

7. CONCLUSION

Two holographic grating samples one plane and one curved were measured in two different laboratories and two different scatterometers. The measurement especially of the curved grating is one of the most demanding tasks in BRDF measurement. The setup has to be perfectly adapted to both the special conditions of a curved sample and a grating.

Holographic gratings often show ring like features and extra peaks that originate in secondary grating structures on top of the designed grating. The illuminating optic of the holographic process is the source of these secondary structures. The quality of the holographic system determines the intensity of the features in the BRDF. For the assessment of the quality of a grating, it is essential to quantify the secondary features.

The results of the 2D measurement of both scatterometers are in good accordance. The calculated equivalent roughness varies by only 5%. The different setups result in some deviations that don't effect the overall result. Drawback of the 2D measurement principle is the impossibility of correctly detecting and discerning of satellites and rings in the BRDF. Dependent on the intensity and position of the features they might not be detectable in a 2D measurement at all.

In 3D measurements, the full features are recorded and peak positions and hights can be correctly determined. Drawback of this method is the long measurement time. The relevant angular area has to be determined and the angular steps in theta and phi have to be adapted to the aperture and angular range. Not all features detected are relevant to system straylight. This is highly dependent on the system and straylight requirements and has to be correlated for each system-grating combination anew. Thorough measurement of the grating BRDF is essential for the compliance status decision of gratings.

In this comparison, only the AlbatrossTT has the facility to measure in 3D and thus could detect quantitatively the rings and satellites around the diffraction peaks of the two holographic gratings.

REFERENCES

[1] B. Harnisch, A. Deep, R.Vink, C. Coatantiec, "Grating Scattering BRDF and Imaging Performances", ICSO 2012, FP 156
[2] Steiner, R., Pesch, A., Erdmann, L. H., Burkhardt, M., Gatto, A., Wipf, R., ... & van den Bosch, B. G. (2013, September). Fabrication of low stray light holographic gratings for space applications. In Imaging Spectrometry XVIII (Vol. 8870, p. 88700H). International Society for Optics and Photonics.
[3] Finck, A., "Table top system for angle resolved light scattering measurement", dissertation at Fakultät für Maschinenbau der Technischen Universität Ilmenau, urn:nbn:de:gbv:ilm1-2014000214 (2014)
[4] S.J. Wein, "Small-Angle scatter measurement", PhD Theses University of Arizona (1989)
[5] M.G.Dittman, "Contamination scatter functions for stray-light analysis", Proc. SPIE Vol. 4774 (2002)
[6] Schröder, S., von Finck, A. and Duparré, A., "Standardization of light scattering measurements", Advanced Optical Technologies. 4(5-6), 361–375, (2015)
[7] Kroneberger, M., Fray, S., "Scattering from reflective diffraction gratings: The challenges of measurement and simulation", Advanced Optical Technologies 6. 10.1515/aot-2017-0032, (2017).
[8] Kroneberger, M., Mezger, A., Volatier, J-B., „Scattering from reflective diffraction gratings: the challenges of measurement and verification", Proc. SPIE 10692, 106920G (15 June 2018)
[9] Kroneberger, M., Mezger, A., Becker, S., „Stray light and ghosts in catadioptric spectrometers: Incorporating grating scatter measurements into simulations and ghost sensitivity into system design", Advanced Optical Technologies, submitted 7/2018